American Journal of Pathology, Vol. 130, No. 3, March 1988

Phenotypic and Genotypic Analysis of a Human Medulloblastoma Cell Line and Transplantable Xenograft (D341 Med) Demonstrating Amplification of c-myc

HENRY S. FRIEDMAN MD, PETER C. BURGER, MD, SANDRA H. BIGNER, MD, JOHN Q. TROJANOWSKI, MD, PhD, GARRETT M. BRODEUR, MD, XUANMIN HE, CAROL J. WIKSTRAND, PhD, JOANNE KURTZBERG, MD, MICHAEL E. BERENS, PhD, EDWARD C. HALPERIN, MD, and DARELL D. BIGNER, MD, PhD

From the Departments of Pediatrics and Pathology (Neuropathology), the Division of Radiation Oncology, and the Preuss Laboratory for Brain Tumor Research, Duke University Medical Center, Durham, North Carolina; the Department of Pediatrics, Washington University School of Medicine, St. Louis, Missouri; the Department of Pathology (Neuropathology), University of Pennsylvania School of Medicine, Philadelphia, Pennsylvania; and the Brain Tumor Research Center, University of California at San Francisco, San Francisco, California

D341 Med is a new continuous cell line and transplantable xenograft derived from a cerebellar medulloblastoma. This line grew *in vitro* in suspension culture with spontaneous macroscopic spheroid formation and demonstrated 20-fold amplification of *c-myc*. Cultured D341 Med cells injected subcutaneously into athymic mice grew as markedly cellular, highly invasive undifferentiated neoplasms. Intracranial tumors grew as markedly cellular mitotically active neoplasms largely located within the subarachnoid space or lining the ventricular system. Immunocytochemical analysis of the cell line and SQ tumors revealed the high (NFP-H) and middle (NFP-M) molecular weight (Mr) neurofilament proteins (NFPs). Immunoblots demonstrated the presence of molecular species that co-migrated with authentic human NFP-H and NFP-M. This cell line and transplantable xenograft may allow, in conjunction with the authors' other models of human medulloblastoma, analysis of the heterogeneous biologic properties and therapeutic sensitivity of this tumor. (Am J Pathol 1988, 130:472–484)

MEDULLOBLASTOMA, the most common malignant brain tumor in childhood, continues to represent a therapeutic challenge. The majority of children with this tumor will ultimately die of progressive disease, despite treatment with increasingly sophisticated surgical and radiotherapeutic intervention.[1] Newer approaches, exploiting advances in rationally designed chemotherapy and monoclonal antibody (MAb) technology, are needed for the effective treatment of this tumor.

Our laboratory has previously reported the establishment and use of two models of human medulloblastoma in the design of rational therapy.[2–4] Medulloblastoma has been studied by many investigators, who have observed marked differences in type and degree of differentiation, tissue pattern, and "grade" of malignancy.[5–11] Models chosen for study of the biologic properties and therapeutic sensitivity of this tumor will need to reflect this spectrum if clinically relevant strategies are to be designed. To date, three continuous human medulloblastoma-derived cell lines and transplantable xenografts have been de-

Supported by NIH Grants CA 11898, CA 36245, CA 44640, 1 NINCDS NS 20023, and 1 K07 NS 00958.

Accepted for publication October 8, 1987.

Address reprint requests to Henry S. Friedman, MD, Department of Pediatrics, Division of Oncology, P.O. Box 2916, Duke University Medical Center, Durham, NC 27710.

scribed,[3,12,13] but this limited number is clearly inadequate to encompass the marked heterogenity of this neoplasm.

We now report the phenotypic and genotypic analysis of a new human medulloblastoma-derived cell line and transplantable xenograft D341 Med, the first to date with amplification of the c-*myc* oncogene. It will add to the cell lines that can be used for study of the biology and therapeutic responsiveness of the medulloblastoma.

Materials and Methods

Clinical History

The patient had been well until 3 5/12 years of age, when signs of increased intracranial pressure appeared and a computerized tomographic (CT) scan of the head revealed a large midline cerebellar mass with obstructive hydrocephalus. The lesion was subtotally excised, and the surgical specimen interpreted histologically as a medulloblastoma. The child was treated with whole neuraxis radiotherapy and did well for 4 months after diagnosis until abdominal distention and ascites developed. A CT scan of the abdomen revealed metastatic lesions, and a bone marrow aspirate revealed 75% replacement with tumor cells. The child died 5 days later; a request for a postmortem examination was denied.

Morphologic Study of the Cerebellar Tumor

A study was made of the cerebellar surgical specimen by light microscopy, including immunohistochemistry for neurofilament protein (NFP, of high [H], middle [M], and low [L] molecular weight) and glial fibrillary acidic protein (GFAP) on paraffin-embedded tissue. The expression of NFP and GFAP was examined with the use of monoclonal antibodies specific for the human forms of these proteins. The preparation and characterization of the MAbs and the procedures for their use as probes in normal and neoplastic human tissues have been described previously.[14-18]

Initiation of Cell Line and Transplantable Xenograft D341 Med

The cell line D341 Med was derived from tumor obtained at craniectomy. This tissue was sterilely sectioned into pieces for cell culture and inoculation into athymic nude mice.

The tissue was mechanically disaggregated and yielded a single cell suspension, plated in 100-mm Petri dishes and T-25 suspension flasks, and incubated at 37 C in a 5% CO_2 in air atmosphere. Adherent cell cultures were fed when the pH of the medium dropped and subcultured at confluence by exposure to 0.12% trypsin and 0.02% EDTA. Suspension cultures were similarly fed and subcultured once to twice weekly. Nonviable cells were removed by density gradient centrifugation through Ficoll-Hypaque (LSM, Organon Teknika Co., Durham, NC). The absence of contamination with mycoplasma was confirmed as previously described.[3]

Growth of Cell Line D341 Med

The population doubling time and colony forming efficiency in soft agar were determined as previously described with Passage 63 and 71 cells, respectively.[2,19]

Phenotypic Analysis of Cell Line D341 Med

The antibodies and antisera used for the *in vitro* studies are listed in Table 1.

Radioimmunoassay (RIA) for Murine Antibodies

The RIA was performed as previously described,[30] with modifications described below for nonadherent cells. The secondary antibody was affinity-purified ^{125}I-labeled goat anti-mouse immunoglobulin (Cooper Biomedical, Inc., Malvern, Pa) diluted in 10% fetal calf serum (FCS): Zinc Option (ZO) medium to give approximately 10^5 cpm/50 μl. Briefly, 2.5×10^5 cells in 25 μl complete medium were plated per well in 96-well assay plates, 50 μl of primary antibody was added, and the plates were incubated at 37 C for 60 minutes. The cells were subsequently washed three times with 10% FCS–0.02% EDTA-ZO by centrifugation and 50 μl of ^{125}I-labeled secondary antibody added to each well. The plates were again incubated at 37 C for 1 hour and finally washed five times with Hanks' buffered saline (HBSS). The cells were removed by exposure to 2 M NaOH and absorption with cotton swabs. The swabs were counted in a Packard Gamma Spectrometer. Results are expressed as the binding ratio (BR), calculated as "exp cpm/bkgd cpm," where "exp cpm" represents the average counts per minute bound by the experimental sample ($n = 3$) and background counts per minute that of P3-63-AG8.4 (IgG) culture supernatant or appropriate subclass of nonreactive immunoglobulin ($n = 3$). A BR ≥ 3.0 is considered positive; such values exceed the mean background value by greater than 3 standard deviations (SD).

Table 1—Monoclonal Antibody Profile for Immunohistochemical Analysis of Cell Line D341 Med

Antibody	Species source	Antigen or immunogen	Reported specificity	Antigen location	Concentration tested	Reference or source
UJ13A	Mouse	Pan-neuro-ectodermal antigen	Normal and tumor tissue of neuroectodermal origin	Cell surface	1.1 μg/ml purified MAb	20 21,22
15E2E2	Mouse	S-100 protein	Cells and tumors of nonectodermal, mesodermal, and epithelial origin	Intracellular	25 μg/ml MAb	23
Anti-NFP	Rat/mouse	Neurofilament	Neuron	Intracellular	1/10 dilution MAb supernatant	15,16,24
Anti-NSE	Rabbit	Neuron-specific enolase	Neuron, reactive astrocytes, astrocytoma, glioblastoma	Intracellular	1/100 dilution antiserum	25 26
Anti GFAP	Mouse	Glial fibrillary acidic protein	Normal, reactive and neoplastic astrocytes	Intracellular	5 ug/ml purified MAb	27
Anti-GS	Rabbit	Glutamine synthetase	Glial cell, astrocytoma	Intracellular	1/100, 1/200 dilution of antiserum	28 29

Indirect Immunfluorescence Assay

The indirect live cell membrane assay was performed as previously described.[31] Briefly, 5×10^5 cells were plated per well in 96-well assay plates and incubated with 50 μl of primary antibody at 4 C for 2 hours. They were washed three times with 10% FCS–0.02% EDTA-ZO medium and incubated with 50 μl of fluorescein-conjugated secondary antibodies of appropriate species specificity at 4 C for 2 hours. The cells were washed as described above and mounted with 50% glycerol in Dulbecco's phosphate-buffered saline (PBS). A minimum of 200 cells per test well were scored for fluorescence under dark field ultraviolet with a Zeiss Universal microscope. The fluorescence index (FI) was calculated as follows: $FI = 100 \times (A - B)/A$, where A is the percentage of nonfluorescing cells with control antibodies, and B the percentage of fluorescing cells with tested MAbs. When cells were tested for expression of intracellular antigen, they were fixed with −20 C acetone for 30 seconds and then tested as described. To examine the distribution of intracellular antigen, we spun the cells onto glass slides by the cytospin technique and fixed and tested them as above.

Growth of Transplantable Xenograft D341 Med in Athymic (Nude) Mice

Animals

Male or female athymic BALB/c mice (nu/nu genotype) 3–4 weeks of age were used, with breeding and husbandary performed as previously described.[32]

Xenograft Establishment

Four animals were given injections in the right cerebral hemisphere with 30 μl (2.1×10^5 cells/mouse) of a single cell suspension in minimal essential medium (MEM) prepared from the cerebellar tumor. Two other animals were injected subcutaneously in the right flank with 200 μl (1.4×10^6 cells/mouse).

Intracranial Xenograft Transplantation

Tumor-bearing animals were killed by cervical dislocation. The intact brain with macroscopic tumor was removed and passed through a 60-mesh cytosieve, washed with ZO-MEM, and given an injection of an equal volume of 7% methyl cellulose (30μl/mouse) intracranially into 6 animals.

Subcutaneous Xenograft Transplantation

Six animals previously conditioned with 5 Gy of total body irradiation (TBI) were injected subcutaneously in the right flank with 250 μl of whole brain–tumor homogenate derived from established intracranial transplants without methyl cellulose. Resulting flank tumors were transplanted subcutaneously into 12 new animals (300 μl/mouse). Six of these 12 animals were previously conditioned with 5 Gy TBI.

Tumorigenicity of Late-Passage Cells

Twelve animals were injected intracranially with 2.3×10^7 cells/mouse from *in vitro* Passage 61.

Morphologic Study of Xenografts

Two subcutaneous and two intracranial passages were studied by light microscopy, electron microscopy, and immunohistochemistry. At the time they were killed, the animals were anesthetized with methoxyflurane and the head perfused through the heart with either 4% glutaraldehyde in cacodylate buffer or Carson's modification of 3.7% buffered formalin fixative. After 5 minutes of perfusion the brains were removed and placed whole in an appropriate fixative for another 2 hours. They were then sectioned in the coronal plane. One mouse with a subcutaneous tumor was lethally anesthetized with ether and was perfused with cold Tris-buffered saline (TBS). The subcutaneous tumor was excised and used for immunoblots (*vide infra*) and for immunoperoxidase studies using the MAbs to different epitopes in NFPs and GFAP. A subcutaneous nodule in a second animal was excised during deep general anesthesia. The lesion was diced into 1-mm cubes in 4% glutaraldehyde and sodium cacodylate buffer. An adjacent 1-cm square block was submitted for paraffin embedding and histologic study.

Immunohistochemical Analysis of Subcutaneous Xenografts and Cultured Cells

Bouin's fixed paraffin sections and frozen sections melted and dried onto glass slides without chemical fixation were used for immunoperoxidase studies with the anti-NFP and anti-GFAP MAbs described above and listed in Table 3. In addition, cultured D341 Med cells were grown, pelleted, and fixed with Bouin's fixative as described earlier.[18] Pellets were also subjected to denaturation by microwave treatment using an Amana Riccar microwave oven at a power level of 8 for 6 minutes in TBS to a temperature of 68 C. These pellets were also embedded in paraffin, and 6-μ-thick sections were cut for immunocytochemical study. Subsequent immunoperoxidase studies were conducted as described earlier.[17]

Immunoblot Analysis of Subcutaneous Xenografts

Immunoblot studies were performed on homogenates of portions of the subcutaneous tumors according to previously described procedures.[17,18] In addition, because the levels of NFPs were relatively low in this medulloblastoma cell line, immunoprecipitated NFPs from the cultured cells were also used for immunoblot analysis. Briefly, 4×10^8 D341 Med cells, grown as described previously,[18] were harvested, washed thrice in TBS with 1 mM EGTA, and homogenized in 4 ml of boiling 1% sodium dodecyl sulfate (SDS) with 0.1 U/ml of aprotinin and 0.5 mM phenylmethylsulfonyl fluoride (PMSF). Samples were boiled for 15 minutes, allowed to cool to room temperature before the addition of a fourfold volume of homogenizing buffer (1% Triton X-100, TBS, 0.1 U/ml aprotinin, 0.5 mM PMSF), and rehomogenized. These homogenates were spun on a microfuge for 5 minutes, and sample supernatants used for immunoprecipitation (3–5 ml of sample supernatant per MAb). Ascitic fluid MAbs diluted 1 : 1000 with the sample supernatants were incubated on a shaker overnight at 4 C. Either goat anti-mouse or goat anti-rat IgG antibodies coupled to agarose (100 μl) were added, and this incubation mixture agitated at room temperature on a shaker for 4 hours. This suspension was washed four times with the homogenizing buffer described above, additionally containing 2 M urea and 0.1% SDS, followed by two additional washes with TBS. Thirty-five microliters of sample buffer were added to the washed agarose mixture, boiled for 5 minutes, and spun for 1 minute on a microfuge. The samples were then subjected to SDS polyacrylamide gel electrophoresis (PAGE), were transferred to nitrocellulose, and underwent subsequent immunoblot analysis as previously described.[17,18]

The MAbs to NFPs used here and for immunocytochemical studies were produced by Lee and coworkers with immunogens from a variety of species[15,16,24]; their specificity for human NFPs has been described in detail.[17] Anti-NFP MAbs are listed in Table 3, together with the immunocytochemical results on sections of the tumor cells. The MAbs to GFAP were produced by Lee et al[14] and Pegram et al[27] and have been shown to be specific for human GFAP as well.[18]

Radiation Technique

Unanesthetized air-breathing animals were irradiated while housed in a specially designed hermetically sealed box. This box fit into a jig attached to a stand-mounted Cobalt 60 source. The roof and floor of the box were designed to provide adequate radiation build-up and back-scatter material. Gamma rays were administered at a source to dorsal surface of the animal distance of 1.58 meters. The total body irradiation dose administered was 5 Gy at a dose rate of 11.9 cGy/min or 4.5 Gy at a dose rate of 24.6 cGy/min. Dose rates were adjusted by the use of a lead attenuator.

Xenograft Measurement Doubling Time and Latency

Subcutaneous tumors were measured, and the doubling time and latency to 500 cu mm were determined as previously described.[2]

Chromosomal Analysis

Chromosomal analysis of the fourth passage subcutaneous tumor and *in vitro* cell line (Passages 10, 27, and 79) were all performed as previously described.[2] The number of chromosomes per cell were counted for at least 16 cells at each passage, and a total of 32 Giemsa-trypsin banded spreads were arranged according to the ISCN nomenclature.[33] The most frequently occurring karyotype at each passage was designated the stemline karyotype.

Molecular Analysis

High-molecular-weight DNA was prepared from a frozen pellet of cultured cells by SDS–proteinase-K lysis and organic extraction as described.[34] DNA was quantitated by a DAPI fluorimetric assay,[35] digested to completion with the restriction enzyme EcoRI (Bethesda Research Laboratories), electrophoresed on a 0.8% agarose gel, and blotted to a nitrocellulose filter. Replicate filters were then hybridized with a radiolabeled probe for N-*myc* (pNb-1)[36] or c-*myc*,[37] washed and exposed to XAR-5 film (Kodak) at −80 C with a lightning plus intensifying screen (duPont). The gene copy number was determined by serial dilution and laser densitometry (LKB Ultroscan Model 2222).

Results

The surgical specimen was a markedly cellular neoplasm of undifferentiated cells with scant cytoplasm (Figure 1). Mitoses were abundant, as were multiple necrotic cells. No regions of fibrillarity, rosettes, or ganglion cells were seen. There were rare strongly GFAP-positive stellate cells in the perivascular regions; however, there was no positive immunostaining of neoplastic cells.

Characteristics of Cell Line D341 Med

The cell line D341 Med has been carried beyond the seventieth *in vitro* passage and is a continuous cell line, as defined by the Committees on Nomenclature of the Tissue Culture Association.[38]

Growth Characteristics

In suspension culture D341 Med grew continuously *in vitro* with macroscopic spheroid formation occurring spontaneously. The population doubling time, calculated from the linear portion of the population growth curve, was 37.4 hours, with a coefficient of correlation of 1.00. Adherent cells of D341 Med grew for only three passages and failed to become established. D341 Med formed colonies in soft agar, with a mean colony-forming efficiency of 3.17% ± 1.28% and a range of 2.2–5.7%.

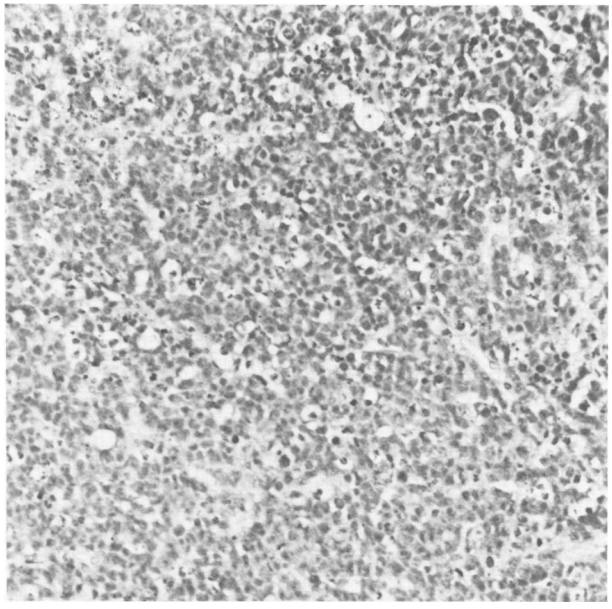

Figure 1—The neoplasm as seen in the initial biopsy specimen from the cerebellum is mitotically active, undifferentiated, and has extensive single-cell necrosis. No rosettes or zones of fibrillarity were present. (H&E, ×170)

Tumorigenicity of Late-Passage Cells (P61)

In all 12 animals given intracranial injections brain tumors developed within 4–6 weeks after injection.

Phenotypic Analysis

The reactivity of the MAbs and monospecific antisera with D341 Med is summarized in Table 2. D341 Med demonstrated expression of the pan-neuroectodermal antigen detected by MAb UJ13A, two of the three NFP subunits, glutamine synthetase and neuron-specific enolase, but neither GFAP nor S-100 protein (Figure 2, Table 3). The blots of the immuno-

Table 2—Phenotypic Analysis of Cell Line D341 Med

Antibody	Binding ratio*	Fluorescence index†
UJ13A (anti-neuroectodermal)	11.6	64
15E2E2 (anti-S-100 protein)	1.4	0
Anti-NSE	ND‡	32
Anti-GFAP§	1.1	1
Anti-GS	ND	30
Anti-NFP	ND	46

*The binding ratio, calculated as experimental counts per minute per background counts per minute, represents the mean of three to five separate experiments; values ≥ 3.0 are considered positive.

†The fluorescence index, calculated as 100 × (A − B)/A, where A is the percentage nonfluorescing cells with control antibodies and B is the percentage of cells fluorescing with the MAb being tested.

‡ND, not done.

§Pegram et al.[27]

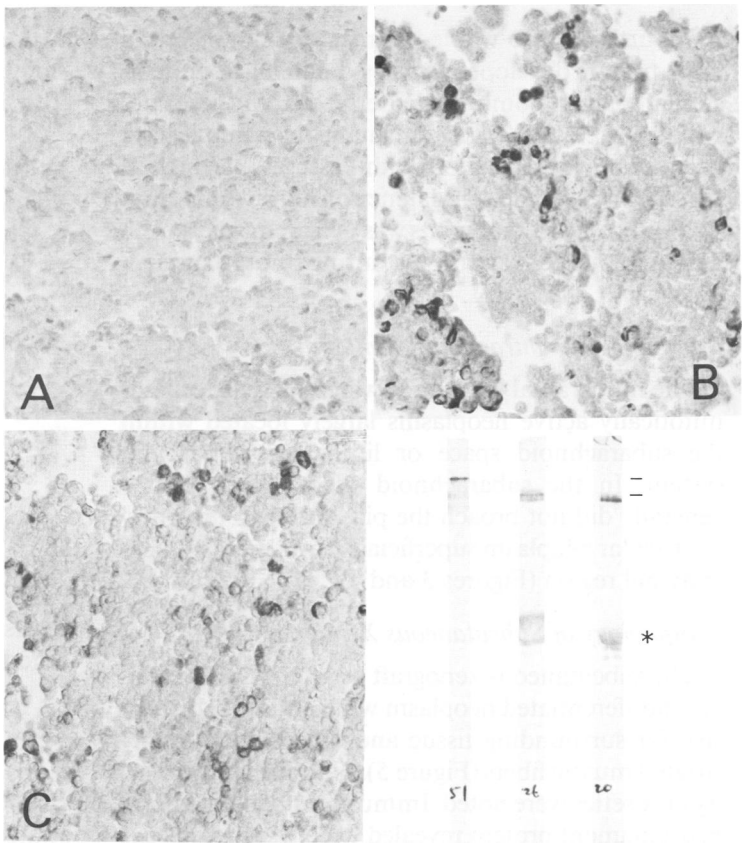

Figure 2—Representative results of immunohistochemical (**A–C**) and immunoblot (**D**) studies conducted on cultured D341 Med cells with MAbs to NFPs and GFAP are illustrated here. The Bouin's-fixed, paraffin-embedded sections of D341 Med cell block shown here were probed with the MAb (2.2B10) to GFAP (**A**), and with monoclonal antibodies to NFPs (RM0254 in **B** and TA50 in **C**). Cytoplasmic NFP immunoreactivity is seen in the tumor cells in **B** and **C**, but none of the tumor cells contain GFAP immunoreactivity (**A**). The sections are lightly counterstained with hematoxylin and enlarged to the same extent (×180). The three nitrocellulose strips in **D** contain D341 Med cell homogenates that were first immunoprecipitated with three different MAbs to NFPs and subjected to SDS-PAGE and electrophoretic transfer to nitrocellulose paper. Then each strip was separately probed with the same MAb used for immunoprecipitation to reveal the presence of NFP-H (left-hand strip) and NFP-M (two right-hand strips). From left to right, the antibodies are TA51, RM026, and DMD020. The *hash marks* on the right indicate the position of NFP-H (*upper hash mark*) and NFP-M (*lower hash mark*). The asterisk identifies the position of the precipitating MAb, which was subjected to SDS-PAGE and electrophoretic transfer to the nitrocellulose paper with the NFPs it precipitated. These bands are lighter in the far left-hand strip because TA51 is a rat immunoglobulin, whereas RM026 and RMD020 are mouse immunoglobulins and mouse PAP reagents that moderately cross-react with rat immunoglobulins were used in the immunoblot procedure.

Table 3—Immunohistochemical Analysis of Cultured D341 Med Cells With Monoclonal Antibodies Specific for Individual Neurofilament or Glial Filament Proteins

Monoclonal antibody	Subunit specificity	Percent positive cells
RMS-12	NFP-L (P-IND)	0
HO-14	NFP-M (P+)	5% or less
RMO-3	NFP-M (P-IND)	5% or less
RMO-123	NFP-M (P+)	5% or less
RMO-254	NFP-M (P-IND)	10% or less
RMO-281	NFP-M (P+)	5% or less
TA-50	NFP-M and NFP-H (P+)	10% less
RMDO-20	NFP-M and NFP-H (P−)	5% or less
HO-57	NFP-H (P+)	25% or less
RMO-24	NFP-H (P+)	0
RMO-217	NFP-H (P+)	0
RMO-304	NFP-H (P−)	0
TA-51	NFP-H (P+)	25% or less*
2.2B-10†	GFAP	0

This table summarizes the results obtained with MAbs to individual NFPs or GFAP with the ABC method and Bouin's-fixed, paraffin-embedded cell blocks. Similar results were obtained with Bouin's-fixed, paraffin-embedded subcutaneous xenografts and cell blocks that were subjected to microwave treatment prior to paraffin embedding. The estimated percentage of cells positive for a given antigen is shown. See Schmidt et al[17] for data on the specificity of these MAbs for human NFPs and for information on the phosphorylation state of the determinants recognized by these MAbs. The phosphorylation state of the epitopes recognized by these MAbs is indicated as follows: P+ means that immunoreactivity is diminished after enzymatic dephosphorylation; P− means that immunoreactivity is increased after the same treatment; P-IND means that this treatment has no effect on the immunoreactivity.

*Cells in mitosis were observed to contain NFP-H immunoreactivity.

†Lee et al.[14]

precipitated cell pellet homogenates revealed molecular species that co-migrated with authentic human NFP-H and NFP-M, obtained postmortem from spinal cord (Figure 2). No GFAP immunobands were detected. Similar results were obtained with immunoblots of the subcutaneous tumor homogenates. NFP-L was not consistently demonstrated in these preparations, although NFP-L positive tumor cells were occasionally seen in sections of the subcutaneous tumor and in sections of the pellets prepared with cultured D341 Med cells.

Characteristics of Transplantable Xenograft D341 Med

Xenograft Establishment and Growth

In all 4 animals given intracranial injections of the cerebellar tumor-derived cell suspension brain tumors developed within 4 weeks after injection. In all 6 animals given the first passage whole-brain tumor homogenate tumors developed within 3–5 weeks. The intracranial tumors have been serially transplanted, with Passage 8 the highest passage level to date. In neither of the 2 animals given subcutaneous injections of primary tumor material did tumors develop.

In all 6 animals given subcutaneous injections of

the fourth-passage whole-brain tumor homogenate, flank tumors developed, as they did in all 12 animals similarly given homogenate derived from these subcutaneous tumors. The subcutaneous tumors have been serially transplanted, with Passage 9 the highest passage level to date. The latency of 500 cu mm tumor size for Passage 5 xenografts was 39.8 ± 6.5 days, with a doubling time, determined during initial exponential growth, of 7.1 ± 1.4 days.

Morphology of Intracranial Xenografts

The intracranial xenografts were markedly cellular mitotically active neoplasms largely located within the subarachnoid space or lining the ventricular system. In the subarachnoid space the neoplasm generally did not broach the pia, although the interventricular neoplasm superficially invaded the subependymal region (Figures 3 and 4).

Morphology of Subcutaneous Xenografts

The subcutaneous xenograft was a markedly cellular undifferentiated neoplasm which was highly invasive for surrounding tissue and incorporated many striated muscle fibers (Figure 5). No zones of fibrillarity or rosettes were noted. Immunohistochemistry for neurofilament protein revealed widely scattered cells with a markedly positive cytoplasmic staining. The staining was largely perinuclear but extended focally into short processes (Figure 6).

Electron Microscopy of Intracranial and Subcutaneous Xenografts

Electron microscopy of the intracranial and subcutaneous xenografts were similar and revealed a markedly cellular neoplasm composed of cells with scant cytoplasm and occasional short bipolar processes (Figure 7). Most of the tumor cells were morphologically undifferentiated, and there were no cell junctions or neurosecretory granules. Approximately 10% of the cells contained small bundles of microtubules. These were apparent either in the perinuclear regions or within the short processes. A rare cell within the intracranial xenograft contained bundles of intermediate filaments in the perinuclear region or in processes. No filament radial arms or cross bridges were noted.

Chromosomal Analysis

In *in vitro* Passage 10, 31 of 50 spreads contained 49 chromosomes. The stemline karyotype as demonstrated in six cells was 49, XY, + 6, + 8, − 22, +

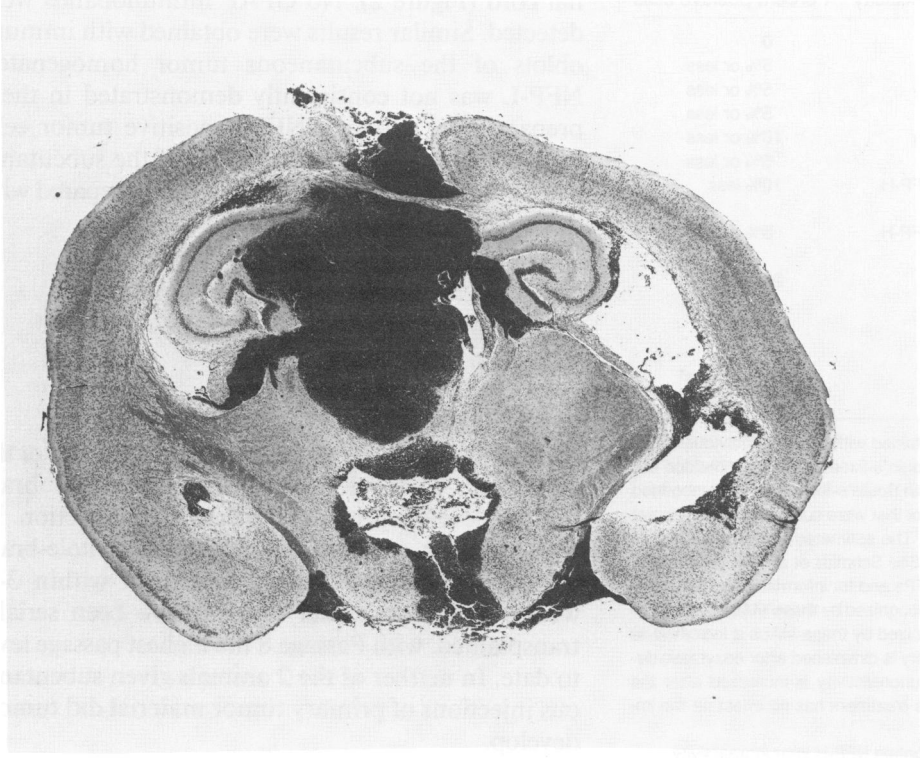

Figure 3—A whole-mount section of the intracranial xenograft demonstrates the markedly cellular neoplasm within the subarachnoid space and walls of the third and lateral ventricles. (H&E, ×250)

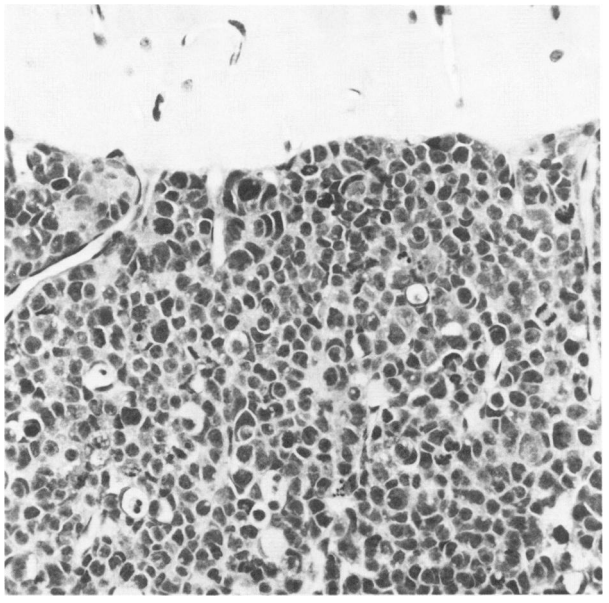

Figure 4—Higher magnification of the intracranial xenograft discloses the undifferentiated mitotically active nature of the neoplasm and its abrupt interphase with the pial surface. (H&E, ×400)

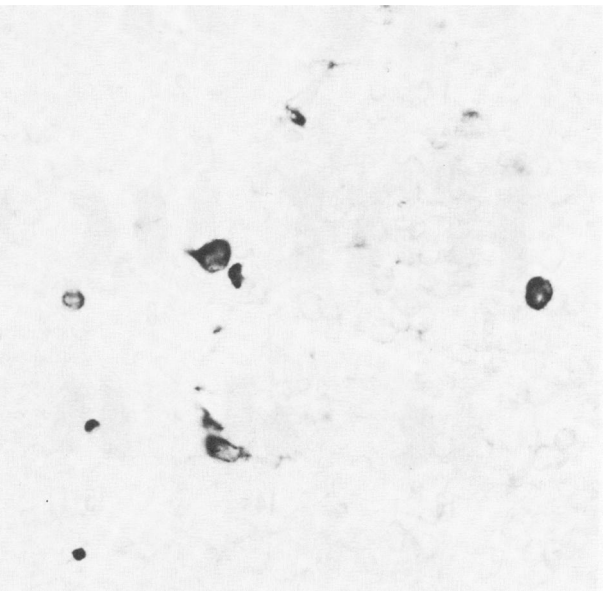

Figure 6—Immunostaining of the subcutaneous xenograft for neurofilament protein discloses scattered markedly positive cells. The staining is largely confined to the immediate perinuclear regions, although at top center the extension into short processes is seen. (×520)

del(1)(p13) + i(17q), + DMs (double minutes). A sideline seen in four karyotyped cells was different from the stemline karyotype only by containing two, rather than three, copies of Chromosome 6. In *in vitro* Passage 27 the original stemline was maintained. By *in vitro* Passage 79, the main population was closely related to the original stemline: S = 47, XY, + 8, − 22, + del(1)(p13), i(17q) + DMs (Figure 8a). Two cells were also identified that possessed the original stemline karyotype. In Passages 10 and 27 virtually every cell contained 20–50 tiny DMs. In *in vitro* p79 approximately 80% of cells contained 20–30 DMs.

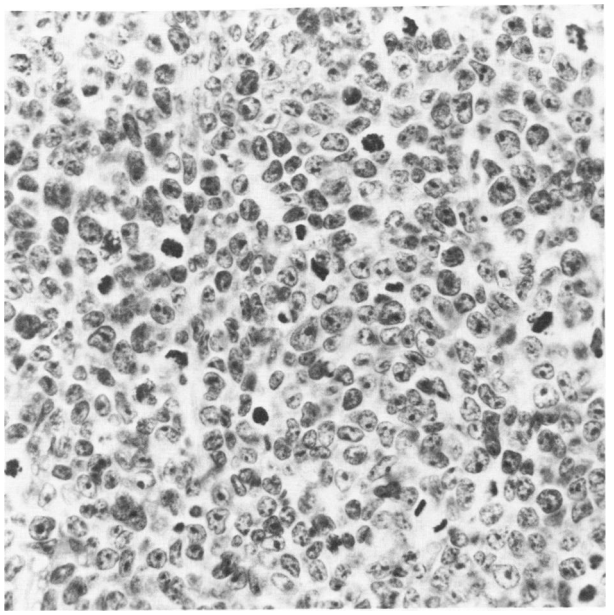

Figure 5—Histologic section of the subcutaneous xenograft discloses an undifferentiated neoplasm, with many mitoses. No evidence of differentiation is seen. (H&E, ×400)

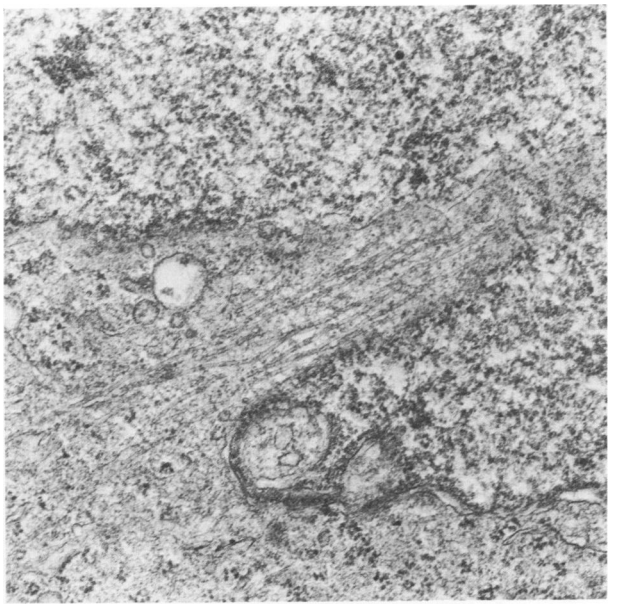

Figure 7—By electron microscopy of both intracranial and subcutaneous xenografts were seen cells that were largely undifferentiated, although scattered small bundles of microtubules were found in a minority of cells. (×30,000)

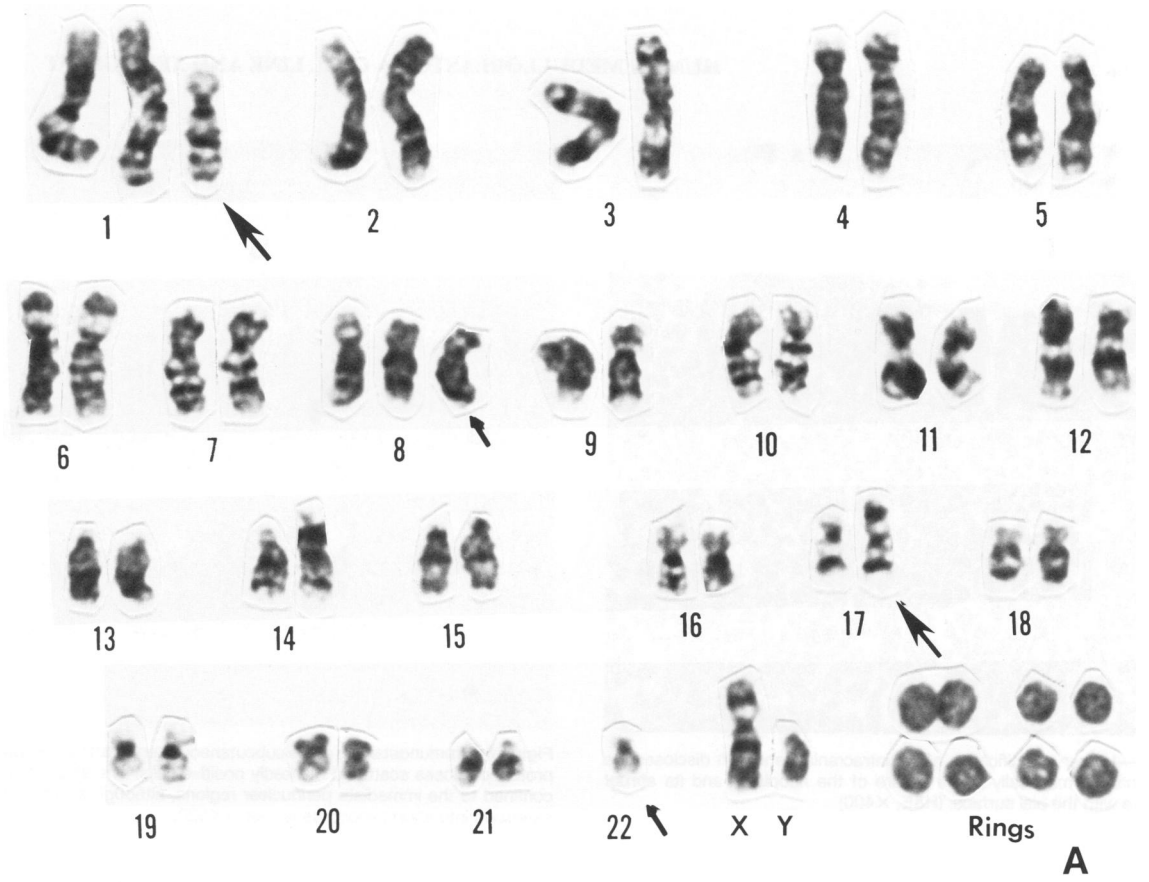

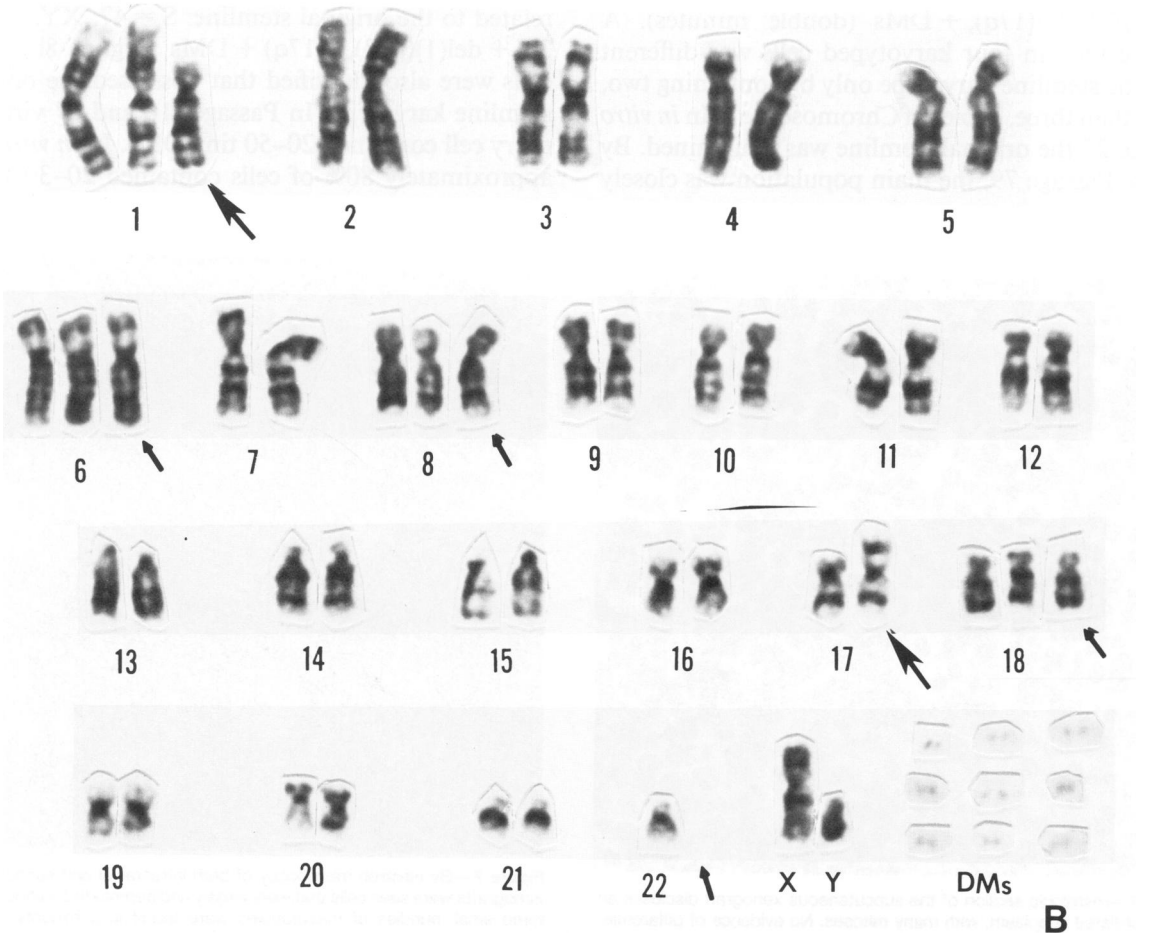

Figure 8A—The stemline karyotype in *in vitro* p79 was 47, XY, + 8, − 22, + del(1)(p13), i(17q), + DMs. In this spread the DMs were large, resembling homogeneously staining rings *Small arrows* indicate numerical deviations; *large arrows* indicate structurally abnormal chromosomes. (Giemsa-trypsin banding, ×1300) **B**—The stemline karyotype in *in vivo* p4 differs from the late *in vitro* pattern shown in **A** only by containing three copies of Chromosomes 6 and 18. Here the DMs are very small. *Small arrows* indicate numerical deviations; *large arrows* indicate structurally abnormal chromosomes. (Giemsa-trypsin banding, ×1300)

They were generally larger and fewer than had been seen originally, occasionally occurring as large, homogeneously staining rings (Figure 8A).

Analysis of cells in the fourth *in vivo* passage revealed the same stemline karyotype as had characterized the early *in vitro* preparation (Figure 8B). Virtually every cell contained 20–50 tiny DMs.

Molecular Genetic Analysis

Figure 9 shows the results of hybridization of the N-*myc* and c-*myc* probes (Figure 9A and B) to DNA from the D341 Med cell line. No increase in gene copy number was seen with the N-*myc* probe. In contrast, the signal intensity was increased approximately 20-fold with the c-*myc* probe, indicating a moderate degree of amplification of this oncogene. Also, no evidence of rearrangement was seen with either of these probes, and no amplification was seen with probes for the oncogenes L-*myc*, c-*erb*B-1, *erb*B-2, c-*sis*, or N-*ras* (data not shown).

Discussion

D341 Med represents a human cell line and transplantable xenograft derived from a cerebellar medulloblastoma, with immunohistochemical and immunoblot detection of two of the three molecular species of NFPs. The ultrastructural characteristics are also consistent with those of a neuroblastic neoplasm. This evidence for neuroblastic differentiation is similar to that seen in D283 Med[3,18] and reflects the potential for expression of neuronal features seen in this neoplasm.[5] Although D283 Med appeared more neuroblastic morphologically by virtue of neuroblastic rosettes and tumor cell processes that contain intermediate filaments with no or infrequent cross bridges, the immunohistochemical and immunoblot detection of NFP in both lines is compelling evidence supporting common neuronal features.

D283 Med cells have been shown to express all three NFPs[18]; we noted that D283 Med cells expressed scant amounts of NFP-L, while D341 Med cells contain no or barely detectable levels of NFP-L. Indeed, D341 Med cells also express relatively less NFP-H and NFP-M than D283 Med cells, as measured by the percentage of tumor cells that express these NFPs. Whether or not the content of NFPs in D341 Med cells reflects a less differentiated (less neuroblastic) stage in the differentiation of medulloblastoma cells, as compared with D283 Med cells, cannot be stated with certainty until detailed studies of the developing human cerebellum are available. Nevertheless, it is interesting that both the morphologic and biochemical evidence supports a less differentiated phenotype for D341 Med cells. Recent studies of the rat nervous system with MAbs used here have shown that NFP expression and phosphorylation are relatively early events in the ontogeny of neurons.[40] Furthermore, NFP-L and NFP-M are expressed prior to NFP-H during normal neurogenesis. Thus, it is likely that the genetic alterations in brain that lead to the development of a medulloblastoma are associated with a disruption in the normal programatic expression of all three NFPs.

These findings can be compared to the only other two published continuous human medulloblastoma cell lines and transplantable xenografts, TE-671[2,12] and Daoy.[13] The phenotypic analysis in our laboratory of these four medulloblastoma cell lines (TE-671, Daoy, D283 Med, and D341 Med) with an extensive

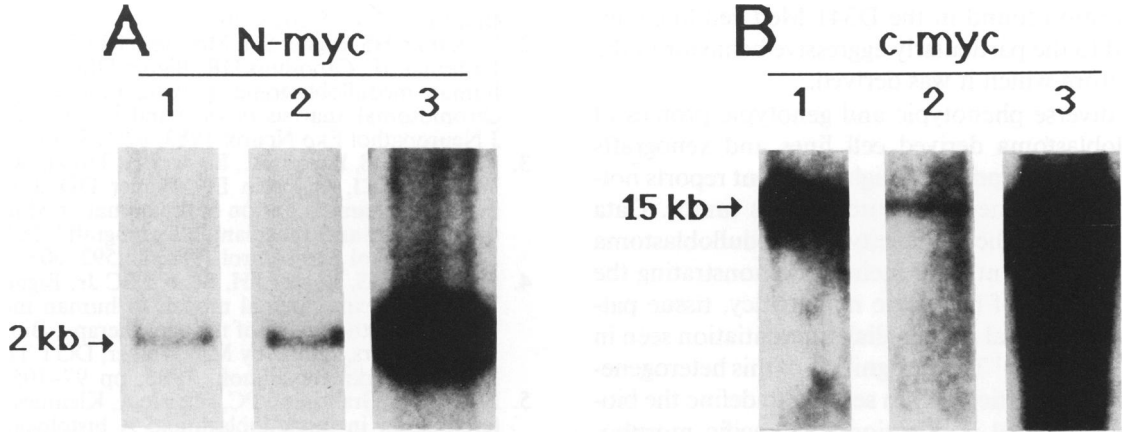

Figure 9—DNA hybridization of DNA from the D341 Med medulloblastoma cell line with radiolabeled probes for N-*myc* (**A**) or c-*myc* (**B**). In both **A** and **B**, Lane 1 is the D341 Med cell line, Lane 2 is a negative control, and Lane 3 is a positive control for hybridization with the respective oncogenes. The positive control for N-*myc* is the NGP cell line,[36] and the positive control for c-*myc* is the COLO-320 cell line.[39] The c-*myc* hybridizations have a high amount of background, due to cross-hybridizing sequences on the probe.[37]

panel of MAbs and monospecific antisera reactive against neuroectodermal, glial-, neuronal-, HLA-A-B-, and lymphoid-associated antigens suggests that there is a spectrum of phenotypic patterns among the four lines, with relative differences in expression of neuronal- or glial-associated antigens, respectively. D341 Med and D283 Med expressed NFP, but did not react with MAbs against GMEM, EGF receptor, HLA-A, B epitopes, B2-microglobulin, or 6/8 of the glioma-associated antigens. TE-671 and Daoy reacted with the MAbs against GMEM, EGF receptor, HLA-A,B epitopes, B2-microglobulins, and 5/8 of the glioma-associated antigens, but did not react with the anti-NFP MAb. Interestingly, these four medulloblastoma cell lines may have patterns of antigen expression *in vitro* that can be distinguished from both glioma and peripheral neuroblastoma (He et al, manuscript in preparation).

Chromosomal analysis of these four medulloblastoma cell lines reveals that D283 Med cells and D341 Med cells demonstrated stem line karyotypes with diploid chromosome counts, while TE-671 cells and Daoy cells demonstrated near tetraploid chromosome counts. No common profile of marker chromosomes is apparent; D341 Med demonstrates 20–50 DMs in virtually all cells. The documentation of DMs in D341 Med suggested the possibility of oncogene amplification, and molecular analysis revealed 20-fold amplification of the c-*myc* oncogene. Thirty percent to 40% of adult gliomas contain amplification of *erb*B, and there are sporadic reports of amplification of c-*myc* and N-*myc* in glial or astrocytic brain tumors and cell lines.[41–45] In addition, there is an interesting report of an amplified and highly expressed gene, *gli,* derived from a human glioma.[46] To date, no consistent pattern has emerged associating amplification of a specific oncogene with a particular type of childhood brain tumor. Nevertheless, it is possible that the c-*myc* amplification found in the D341 Med cell line contributed to the particularly aggressive behavior of the tumor from which it was derived.

The diverse phenotypic and genotypic profiles of medulloblastoma derived cell lines and xenografts should not be surprising in light of recent reports noting the heterogeneous features of this tumor. Data confirming the heterogeneity of medulloblastoma continue to mount, convincingly demonstrating the wide spectrum of histologic malignancy, tissue pattern, and neuronal and/or glial differentiation seen in this neoplasm.[5–11] The recognition of this heterogeneity is critical, particularly in seeking to define the biologic and clinical implications of specific morphologic, phenotypic, or genotypic differences. Recent reports present conflicting interpretations regarding the prognostic importance of morphologic evidence of differentiation. Patients with differentiated neoplasms have been reported to have better[47] and worse[48] prognoses than those with undifferentiated lesions. Although it is reasonable to assume that different cell types or the same cell types with different degrees of differentiation constituting medulloblastoma may demonstrate quite distinct therapeutic profiles, the heterogeneity of medulloblastoma (both between and within individual tumors) limits a precise analysis of these variables.

The very limited material for study of human medulloblastoma (currently limited to four cell lines and xenografts), coupled with the potential scientific advantages associated with its use, supports our continued efforts to establish new medulloblastoma-derived cell lines. These cell lines and xenografts, reflecting the heterogeneity seen in clinical specimens, offer the unique opportunity of addressing phenotypic, genotypic, and therapeutic questions in rigorous controlled studies. The use of well-characterized human medulloblastoma cell lines and xenografts may allow definition of therapeutic interventions whose impact is limited to selective cell types constituting this tumor.

Potential therapeutic benefits include the generation of panels of monoclonal antibodies for use in the diagnosis, localization, and treatment of medulloblastoma (both as tumor tissue and cells exfoliated into the cerebrospinal fluid)[49–53] and the analysis of drug sensitivity, resistance, and delivery in this tumor.[54,55] The ultimate goal of these studies is translation into effective Phase 2 and Phase 3 clinical trials.[56]

References

1. Bloom HJG: Medulloblastoma in children: Increasing survival rates and further prospects. Int J Radiat Oncol Biol Phys 1982, 8:2023–2027
2. Friedman HS, Bigner SH, McComb RD, Schold SC Jr, Pasternak JF, Groothuis DR, Bigner DD: A model for human medulloblastoma: growth, morphology, and chromosomal analysis *in vitro* and in athymic mice. J Neuropathol Exp Neurol 1983, 42:485–503
3. Friedman HS, Burger PC, Bigner SH, Trojanowski JQ, Wikstrand CJ, Halperin EC, Bigner DD: Establishment and characterization of the human medulloblastoma cell line and transplantable xenograft D283MED. J Neuropathol Exp Neurol 1985, 44:592–605
4. Friedman HS, Bigner SH, Schold SC Jr, Bigner DD: The use of experimental models of human medulloblastoma in the design of rational therapy, Biology of Brain Tumors. Edited by MD Walker, DGT Thomas. Boston, Markiners Nijhoff, 1986, pp 97–105
5. Burger PC, Grahmann PC, Bliestle A, Kleihues P: Differentiation in medulloblastoma: A histological and immunohistochemical study. Acta Neuropathol 1987,
6. Rubinstein LJ: The cerebellar medulloblastoma: Its origin, differentiation, morphological variants and bio-

logical behavior, Handbook of Clinical Neurology, Tumors of the Brain and Skull, Part III. Edited by PJ Vincken, GW Bruyn. Amsterdam, North-Holland 1975, 18:167–194
7. Rorke LB: The cerebellar medulloblastoma and its relationship to primitive neuroectodermal tumors. J Neuropathol Exp Neurol 1983, 42:1–15
8. Becker LE, Hinton D: Primitive neuroectodermal tumors of the central nervous system. Hum Pathol 1983, 19:538–550
9. Velasco ME, Ghobrial MW, Ross ER: Neuron specific enolase and neurofilament proteins as markers of differentiation in medulloblastoma. Surg Neurol 1985, 23:177–182
10. Barnard RO, Pambakian H: Astrocytic differentiation in medulloblastoma. J Neurol Neurosurg Psychiatry 1980, 43:1041–1044
11. Sawa H, Takeshita I, Kuramitsu M, Egami H, Fukui M, Sato Y: Neuronal and glial proteins in medulloblastoma: II. Heterotransplantation of human medulloblastoma. Anticancer Res 1986, 6:911–916
12. McAllister RM, Isaacs H, Rongey R, Peer M, Au W, Soukup SW, Gardner MB: Establishment of a human medulloblastoma cell line. Int J Cancer 1977, 20:206–212
13. Jacobsen PF, Jenkyn DJ, Papadimitriou JM: Establishment of a human medulloblastoma cell line and heterotransplantation into nude mice. J Neuropathol Exp Neurol 1985, 44:472–485
14. Lee VM-Y, Page CD, Wu H-L, Schlaepfer WW: Monoclonal antibodies to gel-excised glial filament protein and their reactivities with other intermediate filament proteins. J Neurochem 1984, 42:24–32
15. Lee VM-Y, Carden MJ, Schlaepfer WW: Structural similarities and differences between neurofilament proteins from five different species as revealed using monoclonal antibodies. J Neurosci 1986, 6:2179–2186
16. Lee VM-Y, Carden MJ, Schlaepfer WW, Trojanowski JO: Monoclonal antibodies distinguish several differentially phosphorylated states of the two largest rat neurofilament subunits (NF-H and NF-M) and demonstrate their existence in the normal nervous system of adult rats. J Neurosci 1987, 7:3474–3488
17. Schmidt ML, Carden MJ, Lee VM-Y, Trojanowski JQ: Phosphate dependent and independent neurofilament epitopes in the axonal swellings of patients with motor neuron disease and controls. Lab Invest 1987, 56:282–294
18. Trojanowski JO, Friedman HS, Burger PC, Bigner DD: A rapidly dividing human medulloblastoma cell line (D283 MED) expresses all three neurofilament subunits. Am J Pathol 1987, 126:358–363
19. Bigner DD, Bigner SH, Ponten J, Westermark B, Mahaley MS, Ruoslahti E, Herschman H, Eng LF, Wikstrand CJ: Heterogeneity of genotypic and phenotypic characteristics of fifteen permanent cell lines derived from human gliomas. J Neuropathol Exp Neurol 1981, 15:201–229
20. Allan PM, Garson JA, Harper EI, et al. Biological characterization and clinical applications of a monoclonal antibody recognizing an antigen restricted to neuroectodermal tissues. Int J Cancer 1983, 31:591–598
21. Coakham HB, Garson JA, Brownell B, Kemshead JT: Diagnosis of cerebral neoplasms using monoclonal antibodies. Prog Exp Tumor Res 1985, 29:57–77
22. Coakham HB, Garson JA, Brownell G, Allan PM, Harper EI, Kemshead TT: The use of monoclonal antibodies in the immunohistochemical diagnosis of cerebral and spinal tumors. South Afr J of Surg 1984, 22:13–22
23. Loeffel SC, Gillespie GY, Mirmiran SA, Miller EW, Golden P, Askin FB, Siegal GP: Cellular immunolocalization of S100 protein with fixed tissue sections by monoclonal antibodies. Arch Pathol Lab Med 1985, Med 1985, 109:117–122
24. Lee V, Wu HL, Schlaepeer WW: Monoclonal antibodies recognize individual neurofilament triplet proteins. Proc Natl Acad Sci USA 1982, 79:6089–6092
25. Marangos PF, Zomzely-Neurath C, Luk DCM, York C: Isolation and characterization of the nervous system —specific protein 14-3-2 from rat brain. J Biol Chem 1975, 250:1884–1891
26. Vinores SA, Rubinstein LJ: Simultaneous expression of glial fibrillary acidic (GFA) protein and neuron-specific emolase (NSE) by the same reactive or neoplastic astrocytes. Neuropathol Appl Neurobiol 1985, 11:349–359
27. Pegram CN, Eng LF, Wikstrand CJ, McComb RD, Lee YL, Bigner DD: Monoclonal antibodies reactive with epitopes restricted to glial fibrillary acidic proteins of several species. Neurochem Pathol 1985, 3:119–138
28. Pilkington GJ, Lantos PL: The role of glutamine synthetase in the diagnosis of cerebral tumors. Neuropathol Appl Neurobiol 1982, 8:227–236
29. Dranoff G, Elion GB, Friedman HS, Campbell GL, Bigner DD: Influence of glutamine on the growth of human glioma and medulloblastoma in culture. Cancer Res 1985, 45:4077–4081
30. Wikstrand CJ, Bigner DD: Expression of human fetal brain antigens by human tumors of neuroectodermal origin as defined by monoclonal antibodies. Cancer Res 1982, 42:267–275
31. Wikstrand CJ, Mahaley MS, Bigner DD: Surface antigenic characteristics of human glial brain tumor cells. Cancer Res 1977, 37:4267–4275
32. Bullard DE, Bigner DD: Heterotransplantation of human craniopharyngiomas in athymic "nude" mice. Neurosurgery 1979, 4:308–314
33. ISCN 1985: An International System for Human Cytogenetic Nomenclature. Edited by DG Harnder, HP Klinger. Basel, Karger, 1985
34. Brodeur GM, Seeger RC, Schwab M, Varmus HE, Bishop JM: Amplification of N-*myc* in untreated human neuroblastomas correlates with disease stage. Science 1984, 224:1121–1124
35. Kapuscinski J, Skoczylas B: Simple and rapid fluorimetric method for DNA microassay. Anal Biochem 1977, 83:252–257
36. Schwab M, Alitalo K, Klempnauer KH, Varmus HE, Bishop JM, Gilbert F, Brodeur G, Goldstein M, Trent J: Amplified DNA with limited homology to *myc* cellular oncogene is shared by human neuroblastoma cell lines and a neuroblastoma tumour. Nature 1983, 305:245–248
37. Rothberg PG, Erisman MD, Diehl RE, Rovigatti UG, Astrin SM: Structure and expression of the oncogene c-*myc* in fresh tumor material from patients with hematopoietic malignancies. Mol Cell Biol 1984, 4:1096–1103
38. Shaeffer WI: Proposed usage of animal tissue culture terms. Tissue Culture Association Manual 1978, 4:779–782
39. Alitalo K, Schwab M, Lin CC, Varmus HE, Bishop JM: Homogeneously staining chromosomal regions contain amplified copies of an abundantly expressed cellular oncogene (c-*myc*) in malignant neuroendocrine cells from a human colon carcinoma. Proc Natl Acad Sci USA 1983, 80:707–711
40. Carden MJ, Trojanowski JO, Schlaepfer WW, Lee VM-Y:Two-stage expression of neurofilament polypeptides during rat neurogenesis with early establishment of adult phosphorylation patterns. J Neurosci 1987, 7:3489–3504
41. Libermann TA, Nusbaum HR, Razon N, Kris R, Lax I,

Soreq H, Whittle N, Waterfield MD, Ullrich A, Schlessinger J: Amplification, enhanced expression and possible rearrangement of EGF receptor gene in primary human brain tumours of glial origin. Nature 1985, 313:144–147
42. Wong AJ, Bigner SH, Bigner DD, Kinzler KW, Hamilton SR, Vogelstein B: Increased expression of the EGF receptor gene inmalignant gliomas is invariably associated with gene amplification. Proc Nat Cancer Instit 1987, 84:6899–6903
43. Filmus J, Pollak MN, Cairncross JG, Buick RN: Amplified, overexpressed and rearranged epidermal growth factor receptor gene in a human astrocytoma cell line. Biochem Biophys Res Commun 1985, 131:207–215
44. Garson JA, McIntyre PG, Kemshead JT: N-*myc* amplification in malignant astrocytoma. Lancet 1985, 2:718–719
45. Trent J, Peltzer P, Rosenblum M, Harsh G, Kinzler K, Mashal R, Feinberg A, Vogelstein B: Evidence for rearrangement, amplification and expression of c-*myc* in a human glioblastoma. Proc Natl Acad Sci USA 1986, 83:470–473
46. Kinsler KW, Bigner SH, Bigner DD, Trent JM, Law ML, O'Brien SJ, Wong AJ, Vogelstein B: Identification of an amplified, highly expressed gene in a human glioma. Science 1987, 236:70–73
47. Caputi AJ, McCullough DC, Manz HI, Patterson K, Hammock MK: A review of factors influencing the prognosis of medulloblastoma: The importance of cell differentiation. J Neurosurg 1987, 66:80–87
48. Packer RJ, Sutton LV, Rorke LB, Littman PA, Sposto R, Rosenstock JG, Bruce DA, Schut L: Prognostic importance of cellular differentiation in medulloblastoma of childhood. J Neurosurg 1984, 61:296–301
49. Kemshead JT, Fritschy J, Garson JA: Monoclonal antibody UJ127:11 detects a 220,000-240,000 kdal. glycoprotein present in a sub-set of neuroectodermally derived cells. Int J Cancer 1983, 31:187–195
50. Bullard DE, Adams CJ, Coleman RE, Bigner DD: *In vivo* imaging of intracranial human glioma xenografts comparing specific with nonspecific radiolabeled monoclonal antibodies. J Neurosurg 1986, 64:257–262
51. Coakham HB, Garson JA, Brownell B, Kemshead JT: Diagnosis of cerebral neoplasms using monoclonal antibodies. Prog Exp Tumor Res 1985, 29:57–77
52. Coakham HB, Richardson RB, Davies AG: Antibody guided radiation therapy via the CSF for malignant meningitis. Lancet 1986, 2:860–861
53. Vick WW, Burger SH, Wikstrand CJ, Bullard DE, Kemshead J, Coakham HG, Schlom J, Johnson WW, Bigner DD: The use of a panel of monoclonal antibodies in the evaluation of cytologic specimens from the central nervous system. Acta Cytol 1987, 31:815–824
54. Friedman HS, Colvin OM, Ludeman SM, Schold SC Jr, Boyd VL, Muhlbaier LH, Bigner DD: Experimental chemotherapy of human medulloblastoma with classical alkylators. Cancer Res 1986, 46:2827–2833
55. Friedman HS, Colvin OM, Hilton J, Schold SC, Elion GB, Skapek SX, Blum MR, Savina PM, Muhlbaier LH, Bigner DD: Melphalan cytotoxicity and resistance in medulloblastoma. Proc Am Assoc Cancer Res 1986, 27:381
56. Friedman HS, Mahaley MS, Schold SC Jr, Vick NA, Falletta JM, Bullard DE, D'Souza BJ, Khandekar JD, Lew S, Oakes WJ, Bigner DD: The efficacy of vincrisitine and cyclophosphamide in the therapy of recurrent medulloblastoma. Neurosurgery 1986, 18:335–340

Acknowledgments

Appreciation is expressed to Dr. V. Lee for assistance with the immunoblots and provision of monoclonal antibodies; to T. Skuck, C. Page, G. Ellis, L. Cleveland, and A. Butler for their excellent technical assistance; and to M. Timmons for secretarial assistance.